

# Frequency-resolved photoconductivity in a-As<sub>2</sub>Se<sub>3</sub>Te

R. KAPLAN\*, B. KAPLAN

*Physics Division, Department of Mathematics and Science Education, Education Faculty, University of Mersin, Ciftlikkoy Campus, 33343 Mersin, Turkey*

In-phase and in-quadrature frequency-resolved photocurrent (IP-FRPC and IQ-FRPC) measurements in amorphous (a-) As<sub>2</sub>Se<sub>3</sub>Te thin films are reported as a function of excitation light intensity, wavelength, and applied dc electric field at room temperature. These measurements provide the carrier lifetime distributions directly. The lifetime of a-As<sub>2</sub>Se<sub>3</sub>Te is found to be strongly dependent on excitation light intensity, but to be independent of applied electric field. This is explained in terms of additional gap states which act as recombination centers. We also present the exponent  $\nu$  in the power-law relationship,  $I_{ph} \propto G^\nu$ , between light generation flux and photocurrent at different frequencies and wavelengths. The exponent  $\nu$  is compared for IP-FRPC and IQ-FRPC outputs, and different materials, which supply information about recombination kinetics. We also discuss the results in terms of photocurrent models proposed.

(Received July 3, 2020, accepted November 25, 2020)

**Keywords:** a-As<sub>2</sub>Se<sub>3</sub>Te thin films, IP-FRPC and IQ-FRPC responses, Photocarrier lifetime, Intensity dependence

## 1. Introduction

Chalcogenide glasses are considered to be the subject of a great deal of interest in the study of their basic physics as well as of device technology. They are appropriate material for optical memory disk [1,2], optical elements [3,4] and optical sensors working in the infrared region [5]. Tellurium based-glasses are suitable for the fast and reversible glass to crystal transformation required for optical storage applications such as digital versatile disk technology [6]. Amorphous Te-Se binary system has been studied in both amorphous film and bulk form, due to their electrophotographic applications. For instance, this binary system is used in fiber optics and memory devices [7-8] as they exhibit threshold and memory switching behaviour as well as infrared transmission [9-10].

The optical properties of materials are important to determine their usage in optoelectronic applications. The optical band gap is usually dependent on the defects due to additional elements. The decreasing in direct band gap with increase in thickness is attributed to the formation of some defects leading to an increase in localised states in the band gap. Although the optical properties of a-As<sub>2</sub>Se<sub>3</sub> have been studied, the effect of the addition of Te has not been studied in detail. Therefore the Te based chalcogenide glasses are of particular interest nowadays.

A-As<sub>2</sub>Se<sub>3</sub> thin film glasses have been found to exhibit interesting changes with composition in properties such as the local structure, density, electrical switching behaviour, conductivity activation energy, etc., which have been attributed to the network topological effects. Especially Te-As-Se compositions are perspective materials for manufacturing optical fibers because of their low phonon energy, low optical losses and good thermal and chemical stability.

The optical band gap is reduced by the deposition and diffusion of Te into As<sub>2</sub>Se<sub>3</sub> film which is due to the increase in density of defect states in the gap region. The transmission is decreased, whereas the absorption efficiency is increased with the increase in disorderness.

The variety of light-induced structural transformation in amorphous chalcogenide films is wide and attracts scientific as well as technical interest [11,12]. Among them, photo-induced diffusion has potential application in optoelectronics (photoresists, optical memories, optoelectronic circuits, etc.). The presence of localized states in the gap region is the dominant factor for the photo-induced effects in such type of materials. The lone-pair character of the valence tails leads to very rich behavior under the influence of light. The illumination by band gap light of many amorphous chalcogenides changes their internal and / or surface structure, and the optical absorption edge will have a red or blue shift [13]. To knowledge of the photo-interaction in such films is a crucial point in understanding the basic mechanism and its technological applications such as device making.

Various device applications like rectifiers, photocells, xerography, switching and memory, etc., have made selenium attractive. Unfortunately, pure Se element has disadvantages like short lifetime and low sensitivity [14]. This problem can be overcome by alloying Se with some impurity atoms (As, Te, Bi, Ge, Ga, Sb, etc.), which gives higher sensitivity, higher crystallization temperature and smaller aging effects [11,12]. Chalcogenide glasses in general and vitreous Te-based alloys in particular have been the subject of extensive work, with an emphasis on structure change due to their new technological applications in optical data storage, memory devices, CO<sub>2</sub> detection [15,4]. The addition of an impurity has a pronounced effect on the optical properties of amorphous materials, and this effect can be widely different for

different impurities [16]. Therefore, the ternary compounds involving As-Se-Te have interesting properties as well as technological applications because they form a wide range of glassy region [1].

Photocurrent measurements have been widely used for understanding the defect states in glassy chalcogenides. In most of the chalcogenide glasses, long time exposure to light at room temperature, leads to an appreciable decrease in photocurrent (photodegradation). This is found to be due to the formation of intimate valence alternation pairs under illumination. These defects are stable only at low temperatures and are converted by bond-switching reactions to random pairs of charged defects, known as light induced metastable defects [17,18]. These light induced metastable defects act as electron-hole trapping centers and decrease the photocurrent.

Recombination is a key factor when describing photocarrier transport in chalcogenide glasses because it strongly affects the electrical and optical response of the chalcogenide glass at all levels of external excitation. In order to determine the quality of a semiconductor, an important parameter is the photocarrier lifetime, because it provides information on the distribution of defects exist in the material. The defect and impurity levels affect the carrier lifetime directly by supplying an alternative recombination path or by acting as trapping centers. The carrier lifetime distribution of a material, therefore, provides a sensitive measure of sample quality.

In the present work, we use frequency-resolved photocurrent (FRPC) spectroscopy on a-As<sub>2</sub>Se<sub>3</sub>Te thin films, at different light intensities and applied voltages. The exponent  $\nu$  in the power-law relationship,  $I_{ph} \propto G^\nu$ , between photocurrent and the carrier generation rate is also determined at different frequencies, wavelengths, and materials. The results are discussed in terms of the proposed models that try to explain the photocurrent response in relation to the localized states.

## 2. Experimental details

We produced the thin film of samples of a-As<sub>2</sub>Se<sub>3</sub>Te by using a thermal evaporation unit. The materials used for these samples were from BDH chemicals with a high purity of 99.9992 %. Mostly we put co-planar Al or Au electrodes on the samples by using a suitable Al foil mask and the thermal evaporation unit. However, instead of using a crucible, the Al or Au ingots were evaporated directly from tungsten spiral. For electrode spacing, the different size Cu wires ranging between 0.1 mm and 0.2 mm were used as masks. Copper external leads were contacted with Ag paint. The current-voltage (I-V) measurements taken in dark proved that the contacts were perfectly ohmic. As noted previously [19], gold contacts perform better in injecting hole carriers and thus give larger photocurrents than aluminium contacts for these a-As<sub>2</sub>Se<sub>3</sub>Te chalcogenide samples.

The samples were excited by a HeNe or an Ar laser. An acousto optic modulator (IntraAction Corp., Model AOM-125) was used to modulate the light sinusoidally in

the frequency range of 10 Hz to 100 kHz. The modulation amplitude amounted to 46 % of the bias light intensity. The modulated photocurrent signal excited in this way was measured and analysed by a lock-in amplifier (SR 530 Stanford Research System). The intensity of the excitation light was reduced by neutral density filters.

## 3. Theory

There are many transient photocurrent techniques [20-22] aimed primarily at probing the thermalization of photoexcited carriers in amorphous materials. On a longer time-scale, the decay of the photocurrent in the presence of recombination gives information about both deep recombination centers and traps in thermal equilibrium with the band. The response time is generally measured by measuring the time for the photocurrent to decay to some fraction of its initial value. Measurement of the modulation frequency dependence of the photocurrent is a complementary method of measuring the response time. Oscillatory modulation allows the investigation of details in the steady-state system response, whereas transient decay measurements average over a range of system conditions.

The frequency-resolved photocurrent (FRPC) spectroscopy has already been described [23-25]. In its simplest form, the optical excitation of a sample is modulated with a small amplitude sinusoid and the sample response to this modulation is measured either in-phase or in-quadrature to the phase of the excitation modulation, using a lock-in detection. Logarithmically sweeping the modulation frequency then generates a lifetime distribution directly.

In the mathematical analyses of frequency-resolved spectroscopy (FRS) method, the in-phase FRS gives the integral of lifetime distribution, between the limits  $\tau \sim (2\pi\omega)^{-1}$  and  $\infty$ , while the in-quadrature FRS gives the lifetime distribution directly. For a system with a single characteristic lifetime  $\tau$ , the in-quadrature FRS spectrum is a symmetric band, of half width 0.7 decades peaked at the frequency

$$f_{peak} = \frac{1}{2\pi\tau} . \quad (1)$$

The lock-in output from all lifetime components as the frequency is swept is given by

$$S(\omega) = \int_0^\infty P(\tau) s(\omega, \tau) d\tau \quad (2)$$

where  $P(\tau)$  is the lifetime distribution, and  $s(\omega, \tau)$  is the response function. For quadrature the lock-in response function is given by

$$s(\omega, \tau) = \frac{g_\tau}{(\omega\tau + \frac{1}{\omega\tau})} \quad (3)$$

while in-phase FRS, it takes the following form

$$s(\omega, \tau) = \frac{g_r}{(1 + \omega^2 \tau^2)} \quad (4)$$

where  $g_r$  is the excitation rate. For comparison, the in-quadrature and phase response functions are represented together in Fig. 1. Although the in-quadrature FRS is the most useful form, the in-phase version can also give important additional information on the existence of fast processes beyond the time domain of the in-quadrature measurements. It is worth remembering that if one knows the quadrature response from  $\omega = 0 \rightarrow \infty$  (which one does not), a Kramers-Kronig transform will give the in-phase response. That is all the information is in either response, if complete in  $\omega$ .

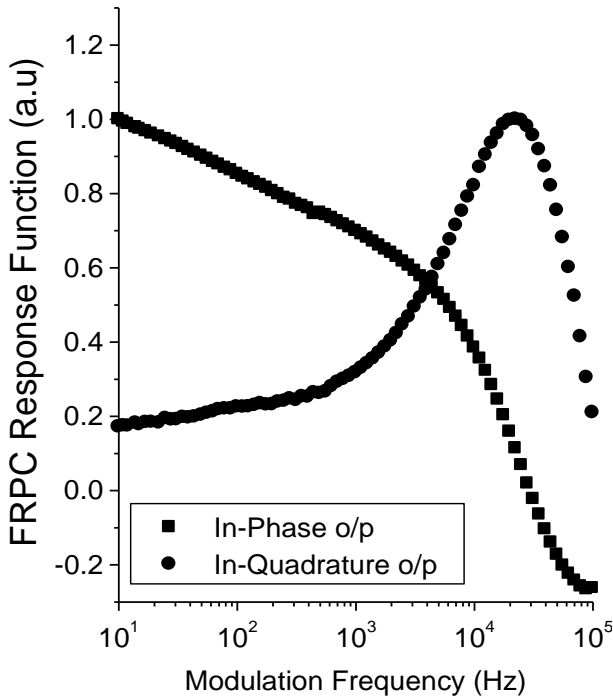


Fig. 1. Frequency-resolved photocurrent (FRPC) response function for the in-quadrature (Eq. (3)) and in-phase (Eq. (4)) of a-As<sub>2</sub>Se<sub>3</sub>Te with a single well defined lifetime. Excitation: HeNe laser (632.8 nm, 2314  $\mu$ W). Applied voltage: 500 V. (a.u, arbitrary units)

#### 4. Results and discussion

The in-phase and in-quadrature frequency-resolved photocurrent (IP-FRPC and IQ-FRPC) responses of the samples in the frequency interval between 10 Hz and 100 kHz were measured as a function of the intensity of the excitation light and applied voltages. Since the energy of the excitation light is much higher than the optical band gap of these materials (1.75 eV), we assume that the carriers are photoexcited between extended states and then a trap limited recombination occurs at room temperature.

Fig. 2 shows IQ-FRPC and IP-FRPC spectra of a-As<sub>2</sub>Se<sub>3</sub>Te for different excitation intensities of HeNe laser

(632.8 nm). Applied voltage was 500 V. As seen from the IQ-FRPC spectra, there is only one single broad spectra in which the peak frequency shifts to lower modulation frequencies with decreasing excitation intensities. This means that there is only one characteristic lifetime.

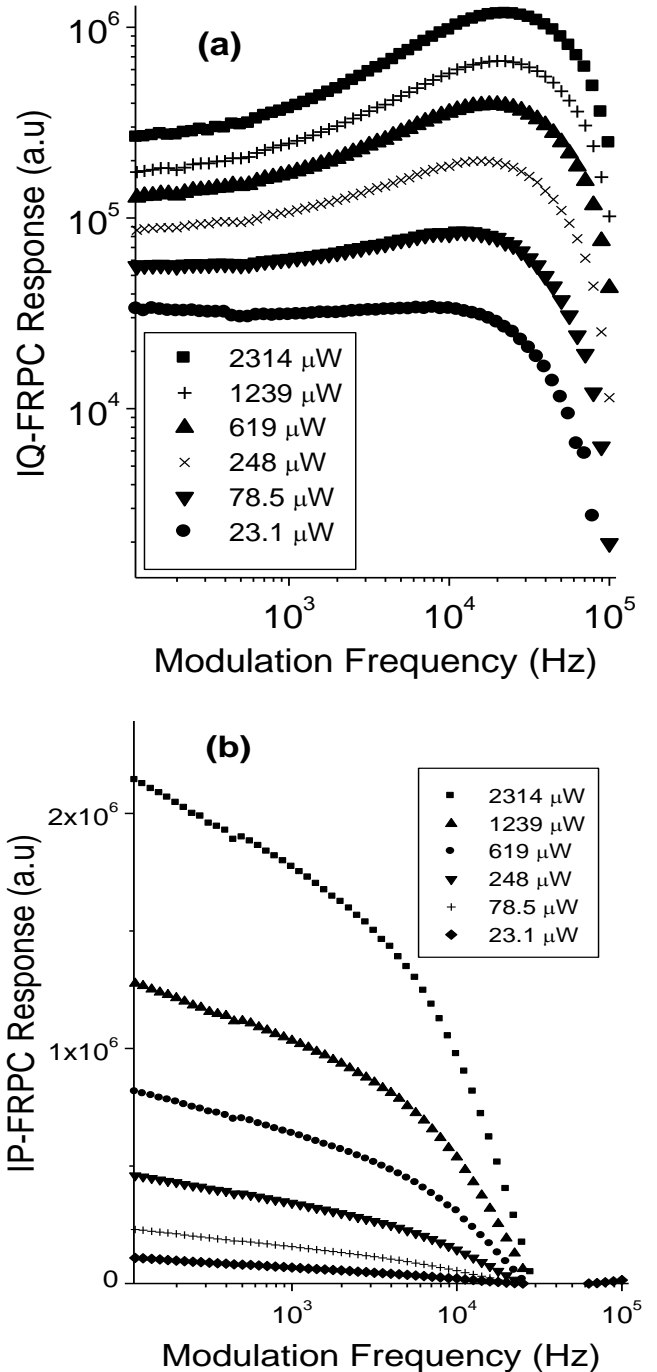


Fig. 2. (a) IQ-FRPC and (b) IP-FRPC spectra of a-As<sub>2</sub>Se<sub>3</sub>Te for different excitation intensities of HeNe laser (632.8 nm). Applied voltage is 500 V

Using Eq. (1), the lifetime  $\tau$  is calculated, and plotted in Fig. 3 as a function of excitation intensity. Obviously the  $\tau$  decreases with increasing excitation intensity. This

decrease is fast below about 200  $\mu\text{W}$ , and above about 1000  $\mu\text{W}$ . This is consistent with a sublinear intensity dependence of the photocurrent. The little variation in lifetime in the range 200 – 1000  $\mu\text{W}$  indicates that free holes are rapidly trapped into the same type of centre in the gap from which electrons can be optically excited.

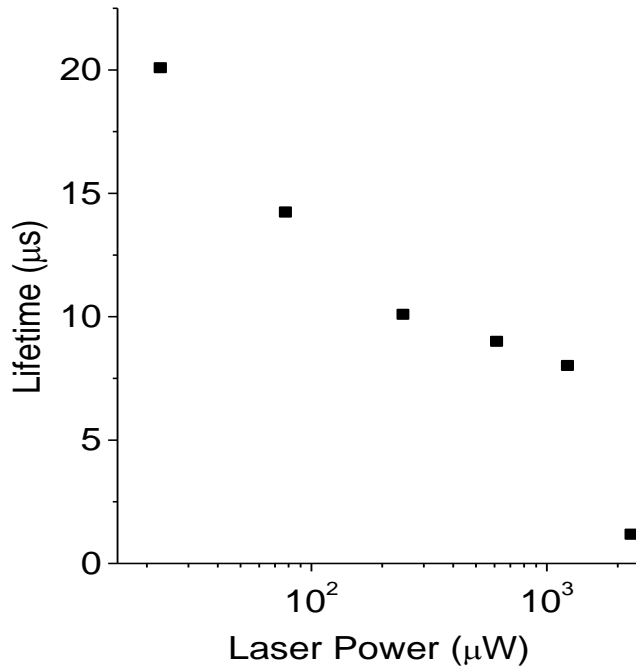


Fig. 3. Excitation intensity dependence of lifetime of  $a\text{-As}_2\text{Se}_3\text{Te}$ .

Fig. 4 shows the effect of applied voltage on the IQ-FRPC and IP-FRPC spectra in  $a\text{-As}_2\text{Se}_3\text{Te}$ . The excitation intensity was 2314  $\mu\text{W}$ , from HeNe laser (632.8 nm). Using the Eq. (1), a lifetime of about 1.13  $\mu\text{s}$  was calculated. However this lifetime is found to be independent of applied voltage and thus electric field. The magnitude of IQ- and IP-FRPC decreases with decreasing voltages as expected. At room temperature, the photocarriers may be thermally ionized from recombination or trapping states, in which only one recombination path is present.

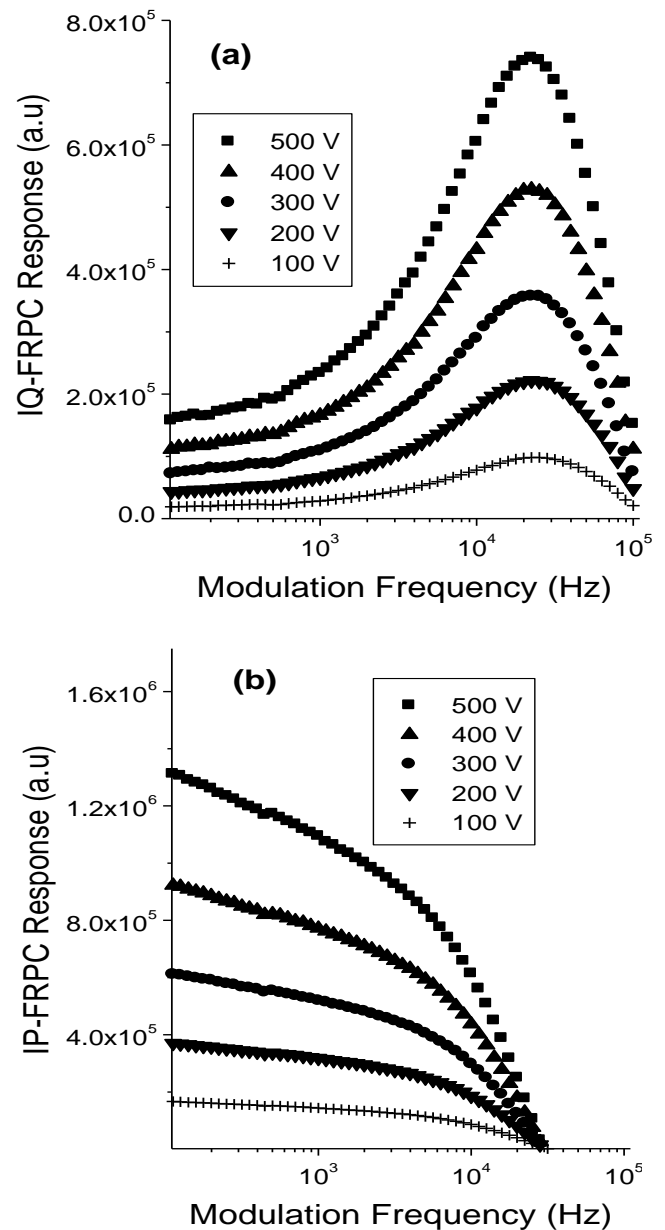


Fig. 4. (a) IQ-FRPC and (b) IP-FRPC spectra in  $a\text{-As}_2\text{Se}_3\text{Te}$  at different applied voltages. Excitation: HeNe (632.8 nm, 2314  $\mu\text{W}$ )

Table 1. Comparison of peak frequencies and carrier lifetimes of different materials under identical conditions. Exc.: HeNe (2314  $\mu\text{W}$ ),  $V_{app} = 500 \text{ V}$ ,  $T = 290 \text{ K}$

Material	a-Se	a-As	a-As <sub>2</sub> Se <sub>3</sub>	a-As <sub>2</sub> Se <sub>3</sub> Te
$f_{peak}$ (Hz)	14125	28183	25118	22387
$\tau$ ( $\mu\text{s}$ )	11.267	5.647	6.336	7.109

In Table 1, we compared the peak frequency and thus the carrier lifetime of different compounds at the same experimental conditions. As seen, a-Se has the largest carrier lifetime, but a-As has the smallest carrier lifetime. The compounds have lifetimes between them as expected.

On the other hand, the addition of Te to the compound of a-As<sub>2</sub>Se<sub>3</sub> increases its carrier lifetime due to the smaller energy band gap of Te (0.32 eV at 300 K).

The next series of our experiments concerns the light intensity dependence of photocurrent,  $I_{ph}$ . For these measurements, the light intensity was increased in steps from 23.1  $\mu$ W up to 2314  $\mu$ W. Fig. 5 shows the light intensity dependence of photocurrent at two different outputs (IP and IQ) and modulation frequencies (10 Hz and 1 kHz). According to the power-law relationship,  $I_{ph} \propto G^\nu$ , between light generation flux and photocurrent, the plot between  $\ln(I_{ph})$  and  $\ln(G)$  should be straight line. The exponent  $\nu$  is calculated from the slope of the curve plotted in Fig. 5. The values of  $\nu$  are found to be close each other (0.5-0.6) for both IP and IQ outputs except for  $\nu = 0.33$  for 10 Hz of IQ. However the result of 10 Hz of IQ for  $\nu$  is not reliable in this type of experiment, so we can not use it due to very small signal detected at this frequency.

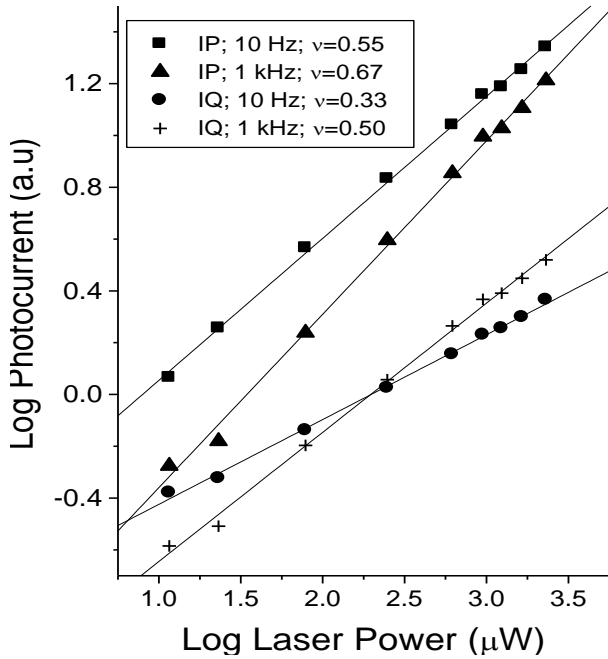


Fig. 5. Excitation (HeNe) intensity dependence of photocurrent of a-As<sub>2</sub>Se<sub>3</sub>Te at different IP and IQ outputs, and frequencies. The calculated values of exponent  $\nu$  in  $I_{ph} \propto G^\nu$  are also shown on the figure

Rose [26] suggests that  $\nu = 1$  corresponds to monomolecular recombination and  $\nu = 0.5$  to bimolecular recombination. However, in the case of continuous distribution of traps the value of  $\nu$  may be anywhere between 0.5 and 1.0 depending on the light intensity and temperature range. As can be seen from Fig. 5, the value of  $\nu$  is close to 0.5-0.6, which corresponds to bimolecular recombination.

It is now well known that the value of the exponent  $\nu$  differs in various materials. In most cases, a sublinear dependence is found and the exponent  $\nu$  in the power-law

relation ( $I_{ph} \propto G^\nu$ ) has quite complicated variations with photon energy, light intensity, temperature and applied field [16]. Fig. 6 shows the excitation wavelength dependence of exponent  $\nu$  for different materials. As will be seen, a-As has the highest  $\nu$  values, a-As<sub>2</sub>Se<sub>3</sub> has the middle  $\nu$  values, and a-As<sub>2</sub>Se<sub>3</sub>Te has the lowest  $\nu$  values for both IP (10 Hz) and IQ (1 kHz) outputs. Also, the  $\nu$  values are different a little and they follow different trends with wavelength for both outputs. There may be a little frequency effect on the  $\nu$  values.

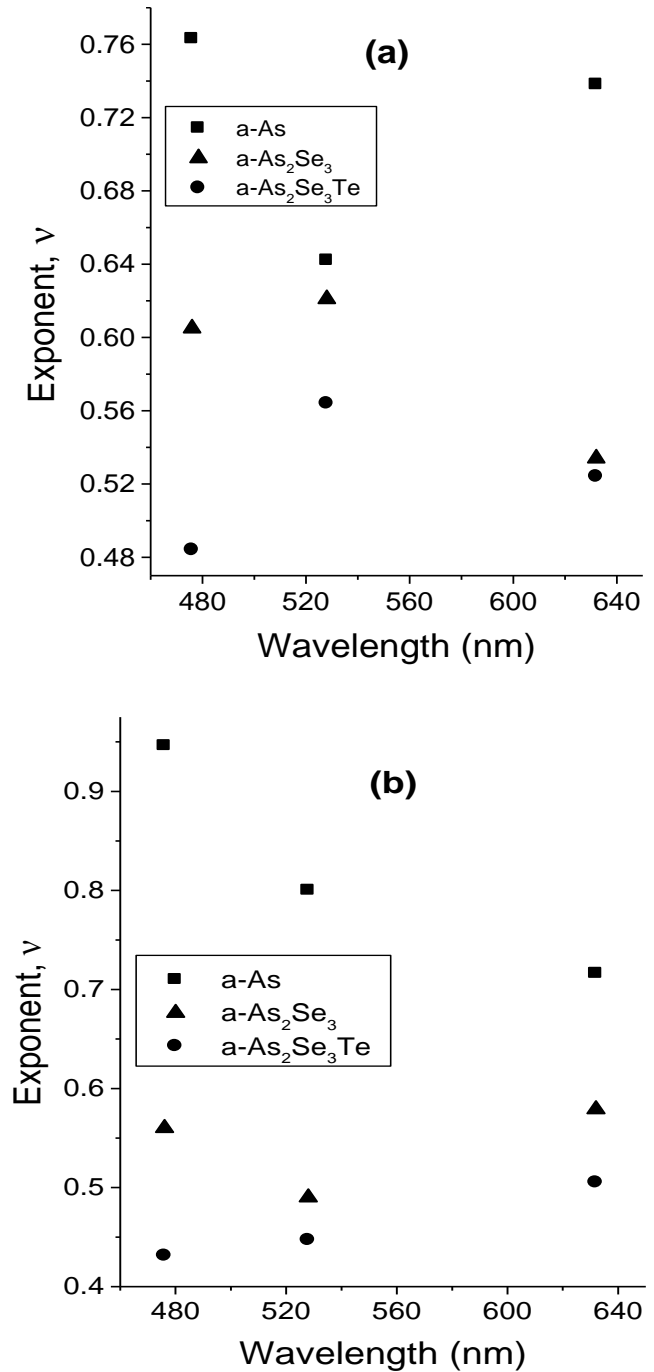


Fig. 6. A comparison of the exponent  $\nu$  as a function of excitation wavelength for different thin film materials used. (a) IP o/p (10 Hz), (b) IQ o/p (1 kHz)

In Fig. 6, the values of exponent  $\nu$  lie between about 0.50 and 0.95, indicating the presence of a continuous distribution of localized states in the energy gap. The exponent  $\nu$  in power-law could qualitatively be associated with the amount of recombination centers located in energy gap; a higher value of  $\nu$ , in general, implies a higher rate of carrier recombination. In this respect, the pure a-As has a larger photocarrier recombination rate than others a-As<sub>2</sub>Se<sub>3</sub> and a-As<sub>2</sub>Se<sub>3</sub>Te due to different wavelength of light absorption. The addition of Se and Te to As increases the charged defects. The intensity and the photon energy dependence at room temperature may be interpreted through the kinetics of photoinduced transitions and thermal relaxations between the extended and localized states, or in terms of the charged defect concept (VAP).

In Fig. 6, when the  $\nu$  values of different compounds are compared, unfortunately they show very complicated behaviours with wavelength for both IP and IQ outputs. However a full interpretation of this result clearly needs a sufficiently detailed knowledge of the recombination mechanism which is not presently available.

## 5. Conclusions

Amorphous semiconductors and in particular chalcogenide glasses are drawing a lot of attention due to manifold applications in different fields. To optimise these materials for possible applications it is essential to understand the carrier lifetime, recombination and transport mechanisms that operate in them. Measurement of photocurrent serves as an important tool to understand the recombination kinetics, which in turn gives information about the localized states present in amorphous semiconductors.

Recombination is influenced both by material properties and by external parameters, such as excitation light intensity, wavelength, and modulation frequency. Especially the recombination lifetime is one of the critical parameters in the search for cost-competitive photovoltaic technologies. Each technology has specific materials issues with respect to the role of recombination lifetime in potential success of that technology. In a-As<sub>2</sub>Se<sub>3</sub>Te, a small single lifetime of 1.13  $\mu$ s was determined for the excitation intensity of 2314  $\mu$ W at room temperature. It is found to be excitation intensity- and material-dependent. It increases with decreasing excitation intensities due to the increase of recombination which is a dominant effect at low light intensities. However, the lifetime is found to be independent of the applied electric field for all compounds used.

We also measured the exponent  $\nu$  in the power-law,  $I_{ph} \propto G^\nu$ . At room temperature the photocurrent is found to be sublinear in photon flux, with the exponent of 0.50-0.67 in the measured frequency and intensity ranges. This result implies that the bimolecular recombination is a dominant effect at room temperature. The exponent,  $\nu$  was also compared for different compounds of a-As, a-As<sub>2</sub>Se<sub>3</sub>

and a-As<sub>2</sub>Se<sub>3</sub>Te under the same experimental conditions. It was found to be excitation wavelength dependent for all materials used. However, IP and IQ outputs of the lock-in amplifier give a little different, but complicated results for  $\nu$ . Despite this, for both outputs, the compound of a-As<sub>2</sub>Se<sub>3</sub>Te has the smallest  $\nu$  values than those of others (a-As and a-As<sub>2</sub>Se<sub>3</sub>) in the whole wavelength range, due to the increase of coordination and light induced defect states in the energy gap. The excitation wavelength dependence of  $\nu$  of the materials used can be related to their light absorption profiles. The larger values of  $\nu$  of a-As and a-As<sub>2</sub>Se<sub>3</sub> show the presence of a continuous distribution of localized states in their band gap.

Our presented results of the carrier lifetime and intensity dependence of photocurrent show that the recombination occurs through the trap states at room temperature. Therefore the release rate from traps controls both the lifetime and photocurrent.

## References

- [1] Z. Wu, Y. Xu, P. Zhang, D. Qi, C. Ma, W. Li, J. Non-Cryst. Solids **527**, 119755 (2020).
- [2] P. R. Sing, M. Zulfequar, A. Kumar, P. K. Dwivedi, J. Non-Cryst. Solids **476**, 46 (2017).
- [3] V. S. Shiryaev, M. F. Churbanov, J. Non-Cryst. Solids **475**, 1 (2017).
- [4] D. Brandova, R. Suoboda, M. Liska, J. Malek, J. Non-Cryst. Solids **475**, 121 (2017).
- [5] N. Mehta, Journal of Scientific and Industrial Research **65**, 777 (2006).
- [6] L. Galvez, E. Lavanant, A. Novikova, C. Goncalvez, B. Bureau, V. Nazabal, T. Jouan, X. H. Zhang, J. Non-Cryst. Solids **480**, 28 (2018).
- [7] B. Karasu, T. Idinak, E. Erkol, A. O. Yanar, El-Cezeri Journal of Science and Engineering **6**(3), 428 (2019).
- [8] D. Biswas, L. S. Sing, A. S. Das, S. Bhattacharya, J. Non-Cryst. Solids **510**, 101 (2019).
- [9] P. Mannu, M. Palanisamy, G. Bangaru, S. Ramakrishnan, A. Kandasami, P. Kumar, Appl. Phys. A **125**, 458 (2019).
- [10] A. Sethi, S. Sharma, Appl. Phys. A **124**, 830 (2018).
- [11] A. A. Al-Ghamdi, Vacuum **80**, 400 (2006).
- [12] M. Saitar, Ledru, A. Hamou, G. Saffarani, Phys. B **245**, 256 (1998).
- [13] J. P. de Neufville, S. C. Moss, S. R. Ovshinsky, J. Non-Cryst. Solids **13**, 191 (1974).
- [14] R. Kaplan, Solar Energy **84**, 401 (2010).
- [15] S. Mauriceon, S. B. Bureau, A. Faber, X. Zhang, W. Geliesen, J. Lucas, J. Non-Cryst. Solids **355**, 2074 (2009).
- [16] R. Kaplan, Sol. Energy Mater. Sol. Cells **85**, 545 (2005).
- [17] K. Shimakawa, A. Kolobov, S. R. Elliott, Adv. Phys. **44**(6), 475 (1995).
- [18] M. S. Iovu, S. D. Shutov, M. Popescu, J. Non-Cryst. Solids **299-302**, 924 (2002).
- [19] J. M. Marshall, A. E. Owen, Philos. Mag. **24**, 1281 (1971).

- 
- [20] S. P. Depinna, D. J. Dunstan, *Phil. Mag. B* **50**, 579 (1984).
- [21] T. M. Searle, *Phil. Mag. Lett.* **61**, 251 (1990).
- [22] C. Main, D. P. Webb, R. Bruggemann, S. Reynolds, *J. Non-Cryst. Solids* **137-138**, 951 (1991).
- [23] D. Wagner, P. Irsigler, D. J. Dunstan, *J. Physics C: Solid State Physics* **17**, 6793 (1984).
- [24] M. A. Lourenco, K. P. Homewood, R. D. McLellan, *J. Appl. Phys.* **73(6)**, 2958 (1993).
- [25] M. A. Lourenco, K. P. Homewood, *Semicond. Sci. Technol.* **8**, 1277 (1993).
- [26] A. Rose, *Concept in photoconductivity and Allied Problems*, Krieger, 1978.

---

\*Corresponding author: ruhikaplan@yahoo.com